

# Multistrange baryon production in relativistic heavy ion collisions

Subrata Pal, C. M. Ko, and Zi-wei Lin

*Cyclotron Institute and Physics Department, Texas A&M University, College Station, Texas 77843-3366*

Using a multiphase transport model, we study the production of multistrange baryons from the hadronic matter formed in relativistic heavy ion collisions. The mechanism we introduce is the strangeness-exchange reactions between antikaons and hyperons. We find that these reactions contribute significantly to the production of multistrange baryons in heavy ion collisions at SPS energies, which has been found to be appreciably enhanced. We have also made predictions for multistrange baryon production in heavy ion collisions at RHIC and found a similar enhancement.

PACS numbers: 25.75.-q, 24.10.Lx

## I. INTRODUCTION

One possible signal for the quark-gluon plasma (QGP) that is expected to be formed in relativistic heavy ion collisions is enhanced production of strange particles [1], particularly those consisting of multistrange quarks such as cascade and omega as well as their antiparticles. The argument is that the rate for strange hadron production is small in hadronic matter due to the large threshold and small cross sections, which is contrary to the large production rate for strange quarks in the quark-gluon plasma [2]. For the lightest strange hadrons such as kaons and antikaons, experiments have shown enhanced production in heavy ion collisions at all energies available from SIS ( $\sim 1A$  GeV) [3], AGS ( $\sim 10A$  GeV) [4], and SPS ( $\sim 158A$  GeV) [5]. Studies based on transport models show that this enhancement can be explained by hadronic scattering alone [6]. However, these models have failed in accounting for the enhanced production of multistrange baryons ( $\Xi, \Omega$ ) by about a factor of three, and the discrepancy is even larger for their antiparticles [7]. To increase the production of these particles requires either to increase the string tension or to decrease the constituent quark mass in the fragmentation of the initial strings in the dense matter [7]. It has also been suggested that the observed enhancement of multistrange baryons and antibaryons may be due to topological defects arising from the formation of disoriented chiral condensate in the initial high density stage of collisions [8]. Of course, the enhancement could simply be a result of the formation of the quark-gluon plasma during collisions. However, to establish strangeness enhancement as a signal for the quark-gluon plasma, we need to exclude any conventional mechanisms. As recently suggested by Vance [9], strangeness-exchange reactions between antikaons and hyperons as well as between their antiparticles can contribute significantly to the production of multistrange baryons and antibaryons in relativistic heavy ion collisions.

In this paper, we shall determine the contribution to multistrange baryon production from the hadronic matter in heavy ion collisions at both SPS and RHIC energies, using a recently developed multiphase transport (AMPT) model [10]. In Section II, we describe briefly the

multiphase transport model. The strangeness-exchange reactions are then discussed in Section III. Results from the AMPT model are given in Section IV B for heavy ion collisions at SPS and in Section IV C for heavy ion collisions at RHIC. Finally, a summary is given in Section V.

## II. MULTIPHASE TRANSPORT MODEL

In the AMPT model, the initial conditions are obtained from the HIJING model [11] by using a Woods-Saxon radial shape for the colliding nuclei and including the nuclear shadowing effect on minijet partons via the gluon recombination mechanism of Mueller-Qiu [12]. After the colliding nuclei pass through each other, the Gyulassy-Wang model [13] is then used to generate the initial space-time information of partons. Subsequent time evolution of the parton phase-space distribution is modeled by Zhang's Parton Cascade (ZPC) [14], which at present includes only the gluon elastic scattering. After minijet partons stop interacting, they combine with their parent strings and are then converted to hadrons using the Lund string fragmentation model [15,16] after an average proper formation time of 0.7 fm/c. Dynamics of the resulting hadronic matter is described by a relativistic transport model (ART) [17].

The parameters in the AMPT model are fixed using the experimental data from central Pb+Pb collisions at center of mass energy of  $17A$  GeV [18]. Specifically, we have included in the Lund string fragmentation model the popcorn mechanism for baryon-antibaryon production in order to describe the measured net baryon rapidity distribution. Also, to account for the pion and enhanced kaon yields, we have modified the values of the parameters in the string fragmentation function. The same parameters are then used to study heavy ion collisions at RHIC energies. The model is able to describe the PHOBOS data [19] for the pseudorapidity distribution of charged particles [20]. Also, the predicted  $\bar{p}/p$  and  $K^-/\pi^-$  ratios are consistent with the data from the STAR [21] and BRAHMS [22] Collaborations. Furthermore, it gives an elliptic flow [23] which is comparable to that measured in the STAR experiment [24].

### III. STRANGENESS-EXCHANGE REACTIONS

To include multistrange baryon and antibaryon production, we consider the following reactions:

$$\bar{K}\Lambda \leftrightarrow \Xi\pi, \quad \bar{K}\Sigma \leftrightarrow \Xi\pi, \quad \text{and} \quad \bar{K}\Xi \leftrightarrow \Omega\pi. \quad (1)$$

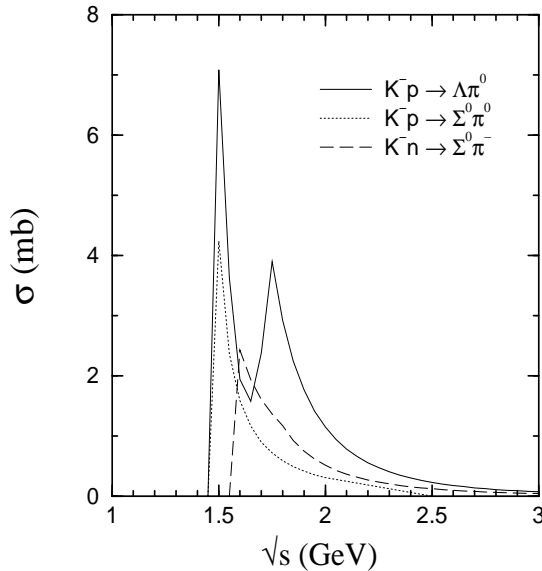


FIG. 1. Experimental cross sections for  $K^-p \rightarrow \Lambda\pi^0$ ,  $K^-p \rightarrow \Sigma^0\pi^0$  and  $K^-n \rightarrow \Sigma^0\pi^-$  as a function of center of mass energy of the interacting antikaon and nucleon.

Since there is no experimental information on these cross sections, we assume that they are the same as the cross section for  $\bar{K}N \rightarrow \Sigma\pi$ , which is the isospin averaged cross section for converting a nucleon to a sigma and can be related to the cross sections for  $K^-p \rightarrow \Sigma^0\pi^0$ , and  $K^-n \rightarrow \Sigma^0\pi^-$  by

$$\sigma_{\bar{K}N \rightarrow \Sigma\pi} = \frac{3}{2}(\sigma_{K^-p \rightarrow \Sigma^0\pi^0} + \sigma_{K^-n \rightarrow \Sigma^0\pi^-}). \quad (2)$$

The cross sections on the right hand side are known empirically and have been parameterized in Ref. [25] as follows,

$$\sigma_{K^-p \rightarrow \Sigma^0\pi^0} = 0.6p^{-1.8} \text{ [mb]}; \quad 0.2 \leq p \leq 1.5 \text{ GeV/c}, \quad (3)$$

$$\sigma_{K^-n \rightarrow \Sigma^0\pi^-} = \begin{cases} 1.2p^{-1.3} \text{ [mb]}, & \text{if } 0.5 \leq p \leq 1 \text{ GeV/c}; \\ 1.2p^{-2.3} \text{ [mb]}, & \text{if } 1 \leq p \leq 6 \text{ GeV/c}. \end{cases} \quad (4)$$

In the above,  $p$  is the  $K^-$  momentum in the laboratory frame. These cross sections are shown in Fig. 1 as functions of center of mass energy of the interacting antikaon and nucleon.

Empirically, the cross section for  $K^-p \rightarrow \Lambda\pi^0$  is also known and has been parameterized [25] as

$$\sigma_{K^-p \rightarrow \Lambda\pi^0} = \begin{cases} 50p^2 - 67p + 24 \text{ [mb]}, & \text{if } 0.2 \leq p \leq 0.9 \text{ GeV/c}; \\ 3p^{-2.6} \text{ [mb]}, & \text{if } 0.9 \leq p \leq 10 \text{ GeV/c}, \end{cases} \quad (5)$$

As shown in Fig. 1,  $\sigma_{K^-p \rightarrow \Lambda\pi^0}$  has a similar magnitude as  $\sigma_{K^-p \rightarrow \Sigma^0\pi^0}$  and  $\sigma_{K^-n \rightarrow \Sigma^0\pi^-}$  except that it has a resonance contribution at  $\sqrt{s} \sim 1.8$  GeV. It may be noted that the channel  $K^-p \rightarrow \Lambda\pi^0$  has resonances while  $\Omega$  has no resonance and the branching ratios of the decay channels for the resonances of  $\Xi$  are not well determined. Therefore for a conservative estimate we assume that the reactions in Eq. (1) are similar to  $\bar{K}N \rightarrow \Sigma\pi$ , which does not show any resonance structure.

We believe the assumption that all strangeness-exchange reaction cross sections have similar magnitudes is reasonable as these reactions are similar except for differences in their particle masses. Justification of this assumption is being studied in an effective hadronic model [26] that is based on SU(3) flavor symmetry. Preliminary results indeed show that the cross sections for these reactions have comparable values.

### IV. MULTISTRANGE BARYON PRODUCTION FROM HEAVY ION COLLISIONS

#### A. Perturbative approach

Since the abundance of multistrange baryons is small in heavy ion collisions, they can be treated perturbatively in the AMPT model as in kaon production from heavy ion collisions at low energies [27], where the collision dynamics is assumed not to be affected by the production of these particles.

First, we consider the process  $\bar{K}\Lambda \rightarrow \Xi\pi$ , in which both  $\bar{K}$  and  $\Lambda$  are treated explicitly, i.e., nonperturbatively, in the AMPT model. The  $\bar{K}\Lambda$  collision is treated by taking their total scattering cross section to be  $\sigma_{\bar{K}\Lambda} = 20$  mb.  $\bar{K}$  and  $\Lambda$  then make a collision if their impact parameter is less than  $\sqrt{\sigma_{\bar{K}\Lambda}/\pi}$ . When this occurs, a  $\Xi$  is produced with a probability given by  $P_{\Xi} = \sigma_{\bar{K}\Lambda \rightarrow \Xi\pi}/\sigma_{\bar{K}\Lambda}$ , which is stored as the  $\Xi$  formation probability. At the same time, both  $\bar{K}$  and  $\Lambda$  have a probability of  $P_{\Xi}$  being destroyed, and a pion is also produced with the same probability. Otherwise, the momenta of  $\bar{K}$  and  $\Lambda$  are changed according to an isotropic distribution.

To treat the inverse reaction of  $\Xi$  absorption by a pion, i.e.,  $\Xi\pi \rightarrow \bar{K}\Lambda$ , we use the cross section determined by detailed balance from Eq. (2). If a collision occurs, the  $\Xi$  is destroyed. The pion has a destruction probability given by the  $\Xi$  formation probability  $P_{\Xi}$  and simultaneously a  $\bar{K}$  and  $\Lambda$  are produced with an isotropic momentum distribution.

The above perturbative approach can be similarly used for the reaction  $\bar{K}\Sigma \leftrightarrow \Xi\pi$ . However, it needs to be modified for the reaction  $\bar{K}\Xi \leftrightarrow \Omega\pi$  as both  $\Xi$  and  $\Omega$  are

treated perturbatively. Again, we take the  $\bar{K}\Xi$  scattering cross section to be  $\sigma_{\bar{K}\Xi} = 20$  mb. Whenever they collide, the  $\Xi$  have a destruction probability given by  $\sigma_{\bar{K}\Xi \rightarrow \Omega\pi}/\sigma_{\bar{K}\Xi}$  while an  $\Omega$  is produced with a probability given by the above probability multiplied by the  $\Xi$  formation probability  $P_{\Xi}$ , which is then stored as the  $\Omega$  formation probability  $P_{\Omega}$ . The destruction of  $\bar{K}$  and simultaneous production of  $\pi$  has a probability of  $P_{\Omega}$ . The inverse reaction  $\Omega\pi \rightarrow \bar{K}\Xi$  can be similarly treated as for  $\Xi\pi \rightarrow \bar{K}\Lambda$ .

## B. Multistrange baryon production at SPS

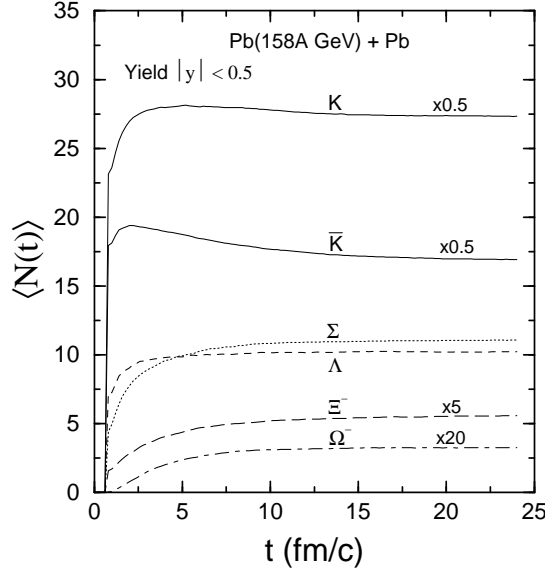


FIG. 2. Time evolution of midrapidity hadrons for Pb+Pb collisions at SPS energy of  $\sqrt{s} = 17A$  GeV at an impact parameter of  $b = 0 - 3$  fm in the AMPT model.

In Fig. 2, we show the time evolution of the abundance of midrapidity kaons (including  $K^*$ ), antikaons (including  $\bar{K}^*$ ),  $\Lambda$ ,  $\Sigma$ ,  $\Xi^-$ , and  $\Omega^-$  in Pb+Pb collisions at  $\sqrt{s} = 17A$  GeV at an impact parameter  $b = 0 - 3$  fm. As is evident from the figure, most multistrange baryons are produced within 10 fm/c after the initial contact of the colliding nuclei when the energy density is high. Compared to the initial yield obtained from HIJING, the dynamical evolution of the system leads to about 30% and 70% increase in the  $\Lambda$  and  $\Xi^-$  production, while most of the  $\Omega^-$ s are produced from hadronic rescattering. Therefore the observed enhancement of multistrange baryons [5] can be largely accounted by the strangeness-exchange reactions in the hadronic matter. Furthermore, the final yield of strange baryons in the AMPT model are in reasonable agreement with that obtained by the WA97 Collaboration [5]. The  $\Omega^-$  production in our model is however a factor of two smaller compared to the data. It may be mentioned that using a rate equation ap-

proach, it was demonstrated [28] that multimesonic reactions  $\bar{Y} + N \leftrightarrow n\pi + nYK$  may lead to an enhanced antistrange hyperon  $\bar{Y}$  production in a purely hadronic scenario. In the present transport model we have neglected these multiparticle reactions which in conjunction with the strangeness-exchange reactions could lead to a better reproduction of the experimental data for multistrange baryons. Alternate to the multiparticle reaction, as for example,  $3\pi + 2\bar{K} \leftrightarrow \Xi + \bar{N}$ , the process  $\bar{K}(\bar{K}^*) + \bar{K}(\bar{K}^*) \leftrightarrow \Xi + \bar{N}$  may be used instead in the transport model to generate  $\Xi$ .

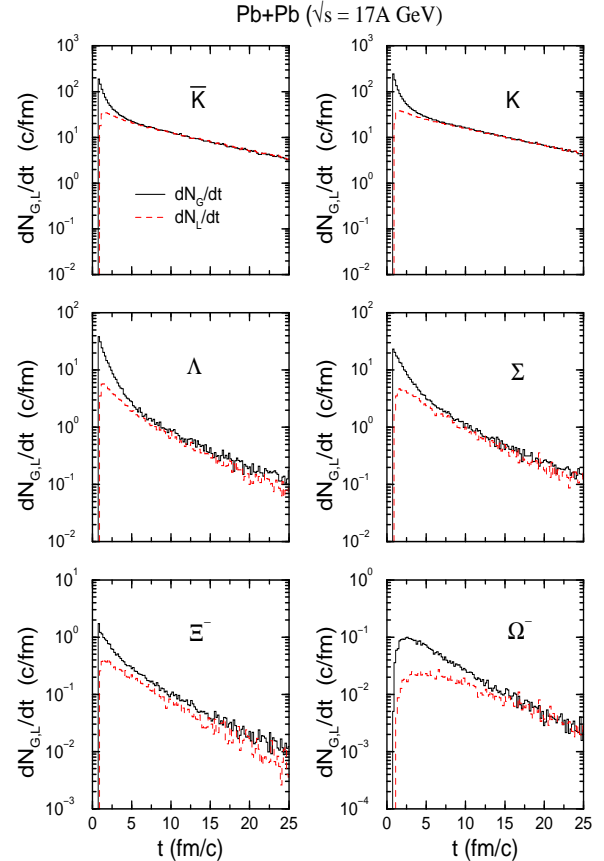


FIG. 3. Production and absorption rates of strange particles in heavy ion collisions at SPS as functions of time.

To see if strange hadrons reach chemical equilibrium in the collisions, we show in Fig. 3 the time evolution of their production (solid lines) and absorption rates (dashed lines). It is seen that most strange particles such as the hyperons and especially the kaons and antikaons approach equilibrium as their production and absorption rates become comparable before the system freezes out. So the abundance of these particles in heavy ion collisions at SPS are consistent with that given by the equilibrium models [29,30].

In Fig. 4 we depict by open circles the transverse mass spectra of hadrons at midrapidity obtained in the AMPT model for the SPS energy. These results are obtained by using mean-field potentials for strange baryons that are

related to the nucleon potential according to their light quark contents. Specifically, relative to the nucleon potential, which is taken to be a stiff Skyrme potential with compressibility of 380 MeV, the lambda and sigma potentials are 2/3, the cascade potential is 1/3, and the omega potential is zero. We see that the theoretical transverse mass spectra of the hadrons agree well with the experimental data shown by solid circles [31,32]. The kaon transverse mass spectrum is however somewhat steeper than the experimental one. This may be due to the weak kaon mean-field potential at high density that is based on the impulse approximation [17] and is used in the present study.

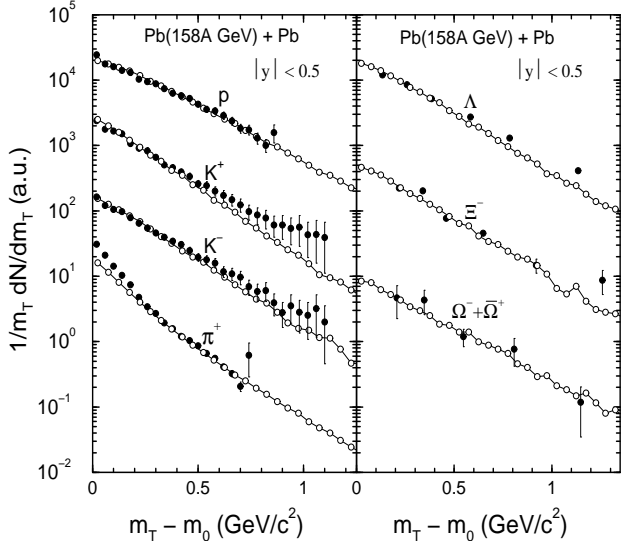


FIG. 4. Transverse mass spectra for midrapidity protons, kaons, antikaons, pions (left panel), and lambda, cascade, omega (right panel) in 158A GeV Pb+Pb central collisions. The solid circles are the experimental data for  $\sim 5\%$  most central collisions from the NA44 Collaboration [31] (left panel), and  $\sim 4\%$  central events from the WA97 Collaboration [32] (right panel). The open circles are the AMPT model calculations for impact parameter of  $b \leq 3$  fm.

The transverse mass spectra can be approximately fitted by an exponential function  $\exp(-m_T/T)$ , where  $T$  is the inverse slope parameter. The slope parameter may provide useful information on the thermal motion and the strong collective transverse flow observed at SPS energy. In Fig. 5, we show the inverse slope parameter of these particles as calculated from the AMPT model (open circles) and compare them with those extracted from the experimental data (solid circles) [32]. The agreement between theory and experiment is reasonable. The linear increase of the inverse slope parameter from pion to kaon and to proton is indicative of the development of collective transverse flow in the system. For nonstrange hadrons,  $T$  may be parametrized by  $T = T_{\text{fo}} + m\langle\beta_t\rangle^2$  (dotted line), where the freeze-out temperature  $T_{\text{fo}} \approx 145$  MeV and average transverse flow  $\langle\beta_t\rangle \simeq 0.39c$ . As in

the experimental data, the inverse slope parameters for strange baryons in the AMPT model are smaller than that for the proton. This is due to both the fact that strange hadrons are produced earlier in the collision when the energy density is high and have smaller scattering cross sections with pions and nucleons than nonstrange hadrons and thus freeze out quite early [33]. Note that for proton with slope parameter  $T = 0.29$  GeV, the contribution from HIJING is about 0.16 GeV, while the mean-field causes a further increase by  $\approx 0.03$  GeV.

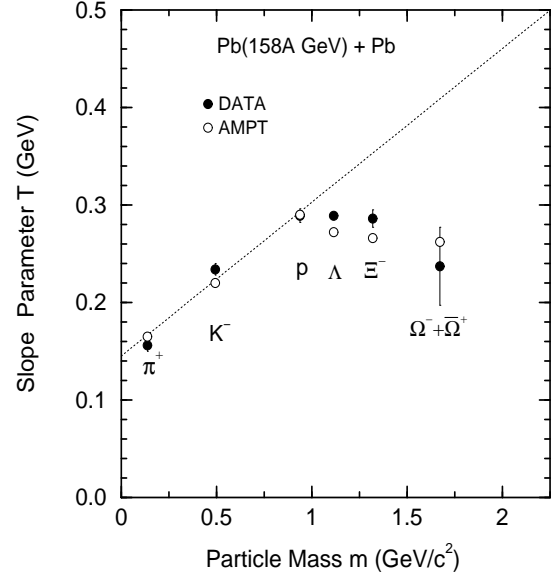


FIG. 5. Inverse slope parameters of various particles in heavy ion collisions at SPS. The open circles are the AMPT calculations and the solid circles are the experimental data [32]. The dotted line represents a linear parameterization (see text).

### C. Multistrange baryon production at RHIC

The predictions of the AMPT model for multistrange baryon production in Au+Au collisions at RHIC energy of  $\sqrt{s} = 130A$  GeV are given in Fig. 6 for their time evolution. Compared to that from heavy ion collisions at SPS, we see that the abundance of the multistrange particles at this RHIC energy is increased by about a factor of two. We have also examined the time evolution of the production and absorption rates of strange particles. It is found that both kaons and antikaons approach chemical equilibrium. On the other hand, strange baryons such as  $\Sigma$  and  $\Xi$  are somewhat out of equilibrium as their production rates are larger than their absorption rates at freeze out. Again, including strange baryon production from multiparticle reactions would lead to chemical equilibrium for these particles as well. Because of its larger absorption cross section by the pion compared to other strange baryons, the  $\Omega$  does reach equilibrium during collision.

We note that our predicted ratios of multistrange baryons to mesons, such as  $\Xi^-/K^-$  and  $\Omega^-/\pi^-$ , are similar to that predicted by the thermal model [34]. In such statistical model analysis of the experimental data at the RHIC energy of  $\sqrt{s} = 130A$  GeV, the hadron yields are in thermal and chemical equilibrium with a baryon chemical potential of  $\mu_B \simeq 51$  MeV and freeze-out temperature of  $T \simeq 175$  MeV. The strangeness-exchange reactions introduced in the present study are thus another mechanism for multistrange baryons to achieve chemical equilibrium in relativistic heavy ion collisions.

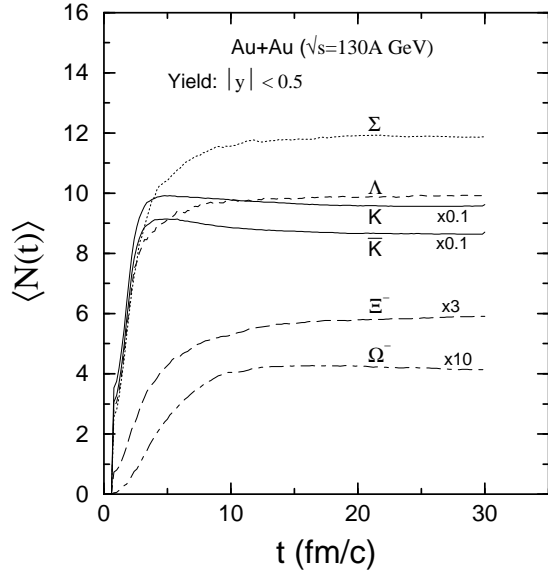


FIG. 6. Time evolution of midrapidity hadrons for Au+Au collisions at RHIC energy of  $\sqrt{s} = 130A$  GeV at an impact parameter of  $b \leq 3$  fm in the AMPT model.

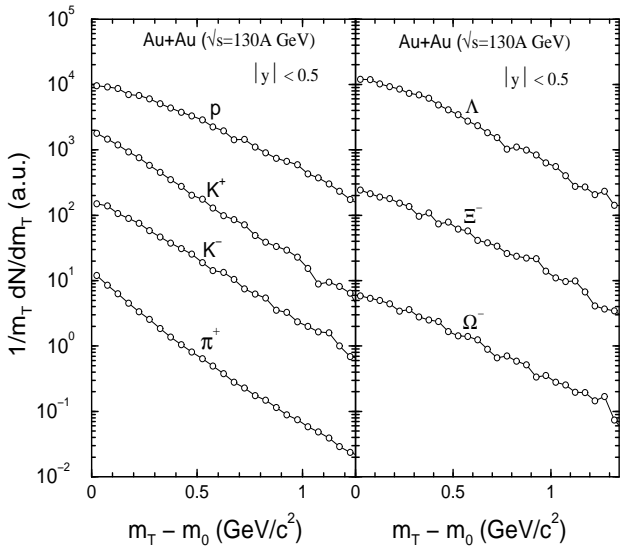


FIG. 7. Same as Fig. 4 but for Au+Au collisions at  $\sqrt{s} = 130A$  GeV for impact parameter of  $b \leq 3$  fm in the AMPT model.

In Fig. 7 we show the transverse mass spectra of midrapidity hadrons for central Au+Au collision at the RHIC energy  $\sqrt{s} = 130A$  GeV. The spectra for protons, pions and kaons are consistent with the preliminary data from the PHENIX Collaboration [35]. The agreement with this data is clearly evident in Fig. 8 where the slope parameters obtained by fitting the spectra in the same  $p_t$  range with the exponential function is depicted. The mass dependence of  $T$  is qualitatively similar to that at SPS energy. At the RHIC energy the slope parameter from pion to proton also exhibits a strong dependence on the particle mass with the freeze-out temperature  $T_{fo} \approx 155$  MeV and the average collective velocity  $\langle \beta_t \rangle \approx 0.43c$ . As at SPS the slope parameter for strange and multistrange baryons reveals a plateau since these particles, mostly generated by strangeness-exchange reactions, are weakly interacting and decouple rather early from the system.

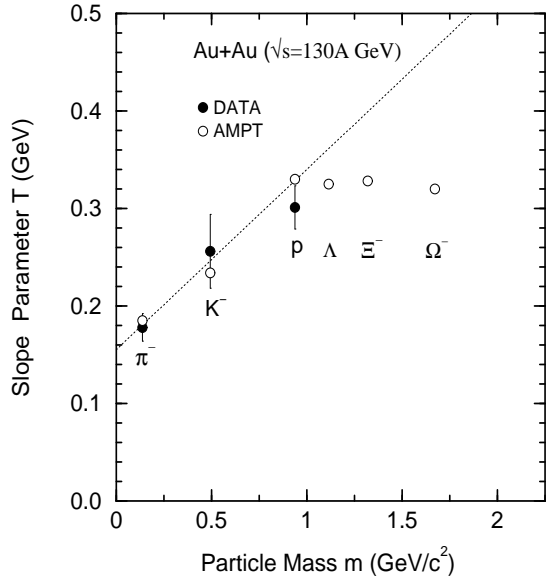


FIG. 8. Inverse slope parameters of various particles in heavy ion collisions at RHIC. The open circles are the AMPT calculations and the solid circles are the experimental data [35]. The dotted line represents a linear parameterization (see text).

## V. SUMMARY

In this paper, we have used a multiphase transport model, that includes both an initial partonic matter and a final hadronic matter, to study the production of multistrange baryons from the strangeness-exchange reactions in the hadronic matter. The cross sections for these reactions are assumed to be the same as the empirically known cross sections for antikaon-nucleon to hyperon-pion. For heavy ion collisions at SPS energies, we find that these reactions lead to an enhanced pro-

duction of multistrange particles, comparable to that observed by the WA97 collaboration. For heavy ion collisions at RHIC, a similar enhancement is obtained from our model. We further find that the slope parameters for the (multi-)strange baryons exhibit a plateau as a function of particle mass at both SPS and RHIC energies.

We have not considered in the present study the hadronic contribution to multistrange antibaryons. For such a study, we need to extend the AMPT model to treat antibaryons similar to that for baryons, which is currently under way.

## ACKNOWLEDGMENT

This work was supported by the National Science Foundation under Grant No. PHY-9870038, the Welch Foundation under Grant No. A-1358, and the Texas Advanced Research Program under Grant No. FY99-010366-0081.

---

[1] J. Rafelski and B. Müller, Phys. Lett. B **101**, 111 (1982).  
[2] P. Koch, B. Müller, and J. Rafelski, Phys. Rep. **142**, 67 (1986).  
[3] D. Miskowiec *et al.*, KaoS Collaboration, Phys. Rev. Lett. **72**, 3650 (1994).  
[4] T. Abbott *et al.*, Phys. Rev. Lett. **64**, 847 (1991); *ibid.* **66**, 1567 (1991).  
[5] E. Anderson *et al.*, (WA97 Collaboration), Phys. Lett. B **433**, 209 (1998); *ibid.* **449**, 401 (1999).  
[6] C.M. Ko and G.Q. Li, J. Phys. G **22**, 1673 (1996); S. Bass *et al.*, Prog. Part. Nucl. Phys. **41**, 225 (1998); W. Cassing and E. Bratkovskaya, Phys. Rep. **308**, 65 (1999).  
[7] S. Soft, S.A. Bass, M. Bleicher, L. Bravina, E. Zabrodin, H. Stöcker, and W. Greiner, Phys. Lett. B **471**, 89 (1999).  
[8] J. I. Kapusta and S.M.H. Wong, nucl-th/0012006.  
[9] S. Vance, nucl-th/0012056.  
[10] B. Zhang, C.M. Ko, B.A. Li, and Z. Lin, Phys. Rev. C **61**, 067901 (2000).  
[11] M. Gyulassy and X.N. Wang, Comp. Phys. Comm. **83**, 307 (1994); X.N. Wang and M. Gyulassy, Phys. Rev. D **44**, 3501 (1991).  
[12] A.H. Mueller and J. Qiu, Nucl. Phys. B **268**, 427 (1986); J. Qiu, Nucl. Phys. B **291**, 746 (1987).  
[13] M. Gyulassy and X.N. Wang, Nucl. Phys. B **420**, 583 (1994).  
[14] B. Zhang, Comp. Phys. Comm. **109**, 193 (1998); M. Gyulassy, Y. Pang and B. Zhang, Nucl. Phys. A **626**, 999 (1997).  
[15] B. Andersson, G. Gustafson, G. Ingelman and T. Sjöstrand, Phys. Rep. **97**, 31 (1983); B. Andersson, G. Gustafson and B. Soderberg, Z. Phys. C **20**, 317 (1983).  
[16] T. Sjöstrand, Comp. Phys. Comm. **82**, 74 (1994).  
[17] B.A. Li and C.M. Ko, Phys. Rev. C **52**, 2037 (1995).  
[18] H. Appelshäuser *et al.* (NA49 Collaboration), Phys. Rev. Lett. **82**, 2471 (1999).  
[19] B.B. Back *et al.* (PHOBOS Collaboration), Phys. Rev. Lett. **85**, 3100 (2000); B.B. Back *et al.* (PHOBOS Collaboration), nucl-ex/0106006.  
[20] Z. Lin, S. Pal, C.M. Ko, B.A. Li, and B. Zhang, Phys. Rev. C **64**, 011902 (2001).  
[21] C. Adler *et al.* (STAR Collaboration), Phys. Rev. Lett. **86**, 4778 (2001).  
[22] I.G. Bearden *et al.* (BRAHMS Collaboration), nucl-ex/0106011.  
[23] Z. Lin *et al.*, in preparation.  
[24] K.H. Ackermann *et al.* (STAR Collaboration), Phys. Rev. Lett. **86**, 402 (2001).  
[25] J. Cugnon, P. Deneye, and J. Vandermeullen, Phys. Rev. C **41**, 1701 (1990).  
[26] C.H. Li, C.M. Ko, and Z.W. Lin, in preparation.  
[27] J. Randrup and C.M. Ko, Nucl. Phys. A **343**, 519 (1980); X.S. Fang, C.M. Ko, and Y.M. Zheng, *ibid.* A **556**, 499 (1993).  
[28] C. Greiner and S. Leupold, nucl-th/0009036.  
[29] P. Braun-Munzinger, I. Heppe, and J. Stachel, Phys. Lett. B **465**, 15 (1999).  
[30] S. Hamieh, K. Redlich, and A. Tounsi, Phys. Lett. B **486**, 61 (2000).  
[31] I.G. Bearden *et al.* (NA44 Collaboration), Phys. Rev. Lett. **78**, 2080 (1997).  
[32] F. Antinori *et al.* (WA97 Collaboration), Eur. Phys. J. C **14**, 633 (2000).  
[33] H. van Hecke, H. Sorge, and N. Xu, Phys. Rev. Lett. **81**, 5764 (1998).  
[34] P. Braun-Munzinger, D. Magestro, K. Redlich, and J. Stachel, hep-ph/0105229.  
[35] J. Velkovska *et al.* (PHENIX Collaboration), nucl-ex/0105012.